Available online at www.eccomasproceedia.org
Eccomas Proceedia COMPDYN (2023) 3677-3690

ECCOMAS
Proceedia

COMPDYN 2023
9th ECCOMAS Thematic Conference on
Computational Methods in Structural Dynamics and Earthquake Engineering
M. Papadrakakis, M. Fragiadakis (eds.)
Athens, Greece, 12-14 June 2023

PROPAGATION OF EPISTEMIC UNCERTAINTY IN MODAL PARAMETERS AND ITS INFLUENCE ON DAMAGE

Saranika Das[1]**, and Koushik Roy**[1]

[1]Department of Civil and Environmental Engineering
Indian Institute of Technology Patna, India
e-mail: koushik@iitp.ac.in

Abstract. *The physical properties of a real structure are stochastic in nature. Mass density, cross-sectional area, Poisson's ratio, modulous of elasticity, etc., develop non-homogeneity in real systems due to spatial distribution. These parameter uncertainties propagate into modal responses involved in structural health monitoring techniques. A detailed literature survey has been performed to identify the suitable probability distribution recommended for defining material uncertainty. Although Gaussian distribution cannot replicate realistic material behaviour, its explicit implementation makes it prevalent. However, based on the principle of maximum entropy, gamma distribution is the appropriate recommendation among all non-Gaussian continuous distributions ranging [0, ∞). In this study, elastic modulous has been considered the primary source of uncertainty. Karhunen–Loève (KL) expansion has been adapted to discretize the stochastic field to determine spectral stiffness of a multi-damaged cantilever bar. Closed-form orthogonal pairs of eigensolutions considering exponential covariance function have been derived. The uncertainty propagation in modal properties have been estimated in both damaged and undamaged system. Extensive simulation studies have been performed to evaluate the effectiveness of the present study.*

Keywords: Uncertainty propagation, Spectral element method, Karhunen–Loève (KL) expansion, Damage quantification.

ISSN:2623-3347 © 2023 The Authors. Published by Eccomas Proceedia.
Peer-review under responsibility of the organizing committee of COMPDYN 2023.
doi: 10.7712/120123.10671.21092

1 INTRODUCTION

The term uncertainty or stochasticity is described as the multiple outcomes of repeated measurements that do not follow any pattern [1]. The sources of uncertainty cannot be limited. Mathematical models, model parameters, numerical algorithms, measurement data are the key sources of uncertainty. In case of uncertainty propagation, tools are developed to obtain the probabilistic descriptions of dynamic responses of any structure depending on the given probabilistic description of system parameters. However, uncertainty quantification is the inverse process in which results obtained from large dataset of identical structures are used to estimate the probability density function (PDF) of the unknown structural parameters. The objectives of stochastic study include understanding the uncertainties inherited by a system, prediction of responses due to various uncertainties, quantification of the confidence interval and minimizing unexpected failures. In this study, modulous of elasticity has been considered as the main source of uncertainty. Now material property being a continuous system parameter, continuous PDFs have been preferred over discrete PDFs for uncertainty modelling.
A detailed literature review of more than hundred science citation indexed (Sci) articles and other documents published in the last two decades (2000-2022) has been performed to identify the best possible PDF recommended for defining material uncertainty in any stochastic study. From Fig. 1(a) it can be observed that priority has been provided to Gaussian, log normal, Weibull and gamma distributions in stochastic modelling of material properties. As there is

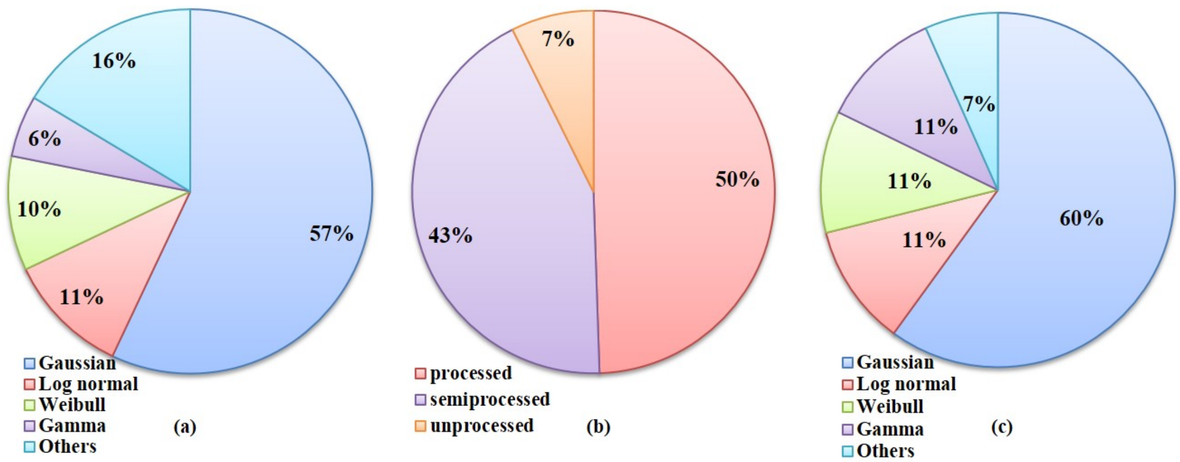

Figure 1: Literature survey (2000-2022): (a) PDFs considered for modelling material uncertainty, (b) types of engineering material and (c) PDFs considered for modelling processed material uncertainty.

no straightforward recommendation of a particular PDF for material uncertainty modelling, to perceive clarity, the dataset of articles has been differentiated into processed or manufactured materials (e.g. steel, aluminium, metals, etc.), semi-processed items (like composites) and unprocessed materials (i.e. concrete, bamboo, etc.). It can be observed from Fig. 1(b) that most of the stochastic study considering material uncertainty has been performed on processed and semi-processed materials. Again, similar trend of adopting various PDFs has been followed as observed in Fig. 1(c) for processed materials. However, there still persists scepticism about the most appropriate PDF for material modelling. The Gaussian distribution function has been prevalently used irrespective of material-type due to its explicit implementation in simulation studies. However, it cannot replicate the realistic behaviour as material property cannot take negative values and its second moment tends to infinity based on the maximum entropy principle [2]. Various studies considering non-Gaussian distribution functions those are valid between 0 to ∞ have been also performed. The application of both normal and log normal distribution function have been discarded [3] stating that the PDF defining material uncertainty must be bounded along with higher moments available. The auto-correlation function must be non-negative and monotonically decreasing function. An approach has been suggested considering beta distribution due to its large variety of shapes. Again gamma distribution has been recommended [4] as it includes other popular distributions like exponential, chi-squared, and Erlang distribution, etc. However, it has been concluded that similar approach may be followed for normal as well as log normal distributions such that it diminishes the importance of considering gamma distribution for the study. Another widely used PDF is the Weibull distribution. Although it has been considered in the studies of ductile materials (e.g. steel) [5] in the initial years of literature considered. However in recent studies, it has been mainly implemented in modelling natural fibers [6] like jute, coconut and for brittle materials [12] especially. Therefore, the Weibull distribution has been discarded from the list of priority of the stochastic study of ductile material. Now in the recent research articles, it has been observed that gamma distribution has been preferred for material uncertainty modelling. The principle of maximum entropy [2] stated that the probability distribution for a positive-valued random variable with a reparameterization leads to gamma distribution. Thus among all the various types of PDFs involved in defining material uncertainty, gamma distribution is the most suitable recommendation to the researchers for the future stochastic studies.

If values of a real variable associated with the outcome of a random experiment such that its values depend on chance, it is called a random variable or a stochastic variable or a variate. If a random variable takes a finite set of values, it is called a discrete variate and if it assumes infinite number of uncountable values, it is called a continuous variate [7]. A random variable is defined by its distribution function and is characterized by its mean and variance. When the quantities vary temporally or spatially, then random process or random field comes into play. Now, any random field can be described as a combination of infinite-dimensional random variables. The vast dimensional problem is difficult to handle by simulation. Thus the dimension need to be truncated to a finite dimension such that the truncated random process turn out to be similar as the original random process with maximum accuracy and minimum computational cost. KL expansion is one of the method for approximation of a random process. It decomposes a random field into finite number of random variables depending on the covariance function considered [8]. In brief, KL expansion discretizes a random process into a series of finite number of orthogonal pairs of eigenvalues and corresponding eigenvectors of the concerned covariance function. This is a sophisticated method. The eigenvalues obtained are gradually decaying such that considering only the higher eigenvalues will estimate the approximated sample space.

In this study, the spectral mass and stiffness of a multi-damaged cantilever bar have been derived. Followed by a detailed mathematical background of KL expansion and estimation of eigensolutions for recreating random field. The spectral stiffness for stochastic condition have been also derived. Further, the application of KL expansion has been described through simulation studies for undamaged cantilever bar considering Gaussian and gamma distribution to evaluate the effectiveness of the present study.

2 MATHEMATICAL ILLUSTRATION ON A CANTILEVER BAR

2.1 Deterministic

An axially vibrating cantilever prismatic bar of length L has been considered as an assembly of N discrete spectral elements of length ϵ each as shown in Fig. 2. The notches between each element indicate the non-propagating cracks. Based on Castigliano's theorem and laws of fracture mechanics, the damages between any p^{th} and $(p+1)^{\text{th}}$ element can be defined by crack flexibility (Θ_p). If there is no damage in between any two segments then the corresponding crack flexibility (Θ_p) is considered to be 0. Therefore, when Θ_p= 0 $\forall$ p =1,2,$\cdots$ $(N-1)$, then the formulation represented undamaged system and for non-zero Θ_p the formulation modifies to damaged system. The spectral deformation ($\widehat{u}_p(x,\omega)$) at any location of the p^{th} spectral element of the system can be given as,

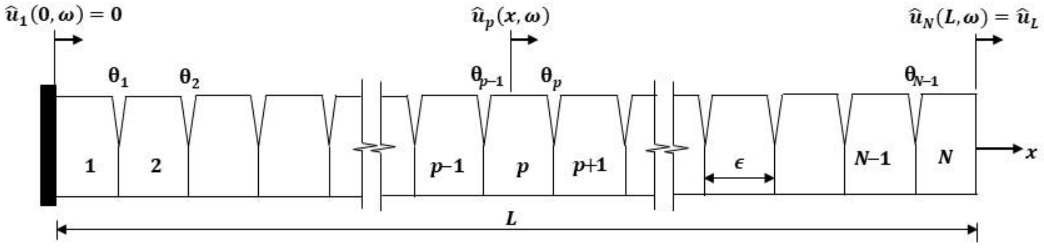

Figure 2: One end restrained axially vibrating prismatic bar having multiple damages $(\Theta_1, \Theta_2, \ldots, \Theta_p, \ldots, \Theta_{N-1})$ uniformly discretized into N spectral elements

$$\widehat{u}_p(x,\omega) = \left\{ e^{ikx} \quad e^{-ik(p\epsilon - x)} \right\} \begin{Bmatrix} a_{2p-1} \\ a_{2p} \end{Bmatrix} = s_p(x,\omega)\widehat{a}_p \quad , \text{for } (p-1)\epsilon \leq x \leq p\epsilon$$

where, x is distance of any location on the bar from the fixed-end and $k = \frac{\omega}{c}$ is wavenumber corresponding to longitudinal wave propagation. $s_p(x,\omega)$ and $\widehat{a}_p$ are spectral shape function matrix and coefficient matrix respectively corresponding to the p^{th} element. Here, i represents unit imaginary number $\sqrt{-1}$. The spectral deformation $\widehat{u}(x,\omega)$ of the total system can be represented in a matrix form as,

$$\widehat{u}(x,\omega) = \begin{Bmatrix} \widehat{u}_1(x,\omega) \\ \vdots \\ \widehat{u}_p(x,\omega) \\ \vdots \\ \widehat{u}_N(x,\omega) \end{Bmatrix} = \begin{bmatrix} s_1(x,\omega) & \cdots & 0 \\ \vdots & \ddots & \vdots \\ \vdots & s_p(x,\omega) & \vdots \\ \vdots & \ddots & \vdots \\ 0 & \cdots & s_N(x,\omega) \end{bmatrix} \begin{Bmatrix} \widehat{a}_1 \\ \vdots \\ \widehat{a}_p \\ \vdots \\ \widehat{a}_N \end{Bmatrix} = S(x,\omega)\widehat{a} \tag{1}$$

To obtain the coefficient matrix $\widehat{a}$, the boundary and compatibility conditions need to be applied. For a fixed-free system, the boundary conditions include

$$\widehat{u}_1(0,\omega) = 0 \tag{2a}$$

$$\widehat{u}_N(N\epsilon,\omega) = \widehat{u}_L \tag{2b}$$

Again, for any intermediate damage between elements p and $(p{+}1)$, the compatibility equations are given as,

$$\widehat{u}_{p+1}(p\epsilon,\omega) - \widehat{u}_p(p\epsilon,\omega) = \Theta_p \frac{\partial \widehat{u}_p(p\epsilon)}{\partial x} \tag{3a}$$

$$\frac{\partial \widehat{u}_p(p\epsilon)}{\partial x} = \frac{\partial \widehat{u}_{p+1}(p\epsilon)}{\partial x} \tag{3b}$$

where, Θ_p indicates crack flexibility corresponding to damage between p^{th} and $(p{+}1)^{\text{th}}$ element. Combining Eqs. (1-3), the nodal spectral displacements $\widehat{u}_{\text{node}}$ can be expressed as

$$\widehat{G}\,\widehat{a} = \widehat{u}_{\text{node}} \tag{4}$$

where, $\widehat{a} = \{\widehat{a}_1, \widehat{a}_2, \cdots, \widehat{a}_{2N-1}, \widehat{a}_{2N}\}^T_{2N\times 1}$, $\widehat{u}_{\text{node}} = \{0, 0, \cdots, 0, \widehat{u}_L\}^T_{2N\times 1}$ and $\widehat{G}$ can be expressed as,

$$\begin{bmatrix}
1 & e^{-ik\epsilon} & 0 & 0 & 0 & \cdots & \cdots & \cdots & \cdots & \cdots & \cdots & \cdots & 0 \\
(ik\Theta_1-1)e^{-ik\epsilon} & -(ik\Theta_1+1) & e^{-ik\epsilon} & e^{-ik\epsilon} & 0 & \cdots & \cdots & \cdots & \cdots & \cdots & \cdots & \cdots & 0 \\
-ike^{-ik\epsilon} & ik & ike^{-ik\epsilon} & -ike^{-ik\epsilon} & 0 & \cdots & \cdots & \cdots & \cdots & \cdots & \cdots & \cdots & \vdots \\
\ddots & \ddots & \ddots & \ddots & \ddots & \ddots & \ddots & \ddots & \ddots & \ddots & \ddots & \ddots & \vdots \\
0 & \cdots & \cdots & \cdots & 0 & (ik\Theta_p-1)e^{-ikp\epsilon} & -(ik\Theta_p+1) & e^{-ikp\epsilon} & e^{-ik\epsilon} & 0 & \cdots & \cdots & 0 \\
\vdots & \cdots & \cdots & \cdots & 0 & -ike^{-ikp\epsilon} & ik & ike^{ikp\epsilon} & ike^{ik\epsilon} & 0 & \cdots & \cdots & \vdots \\
\vdots & \cdots & \cdots & \cdots & \cdots & \ddots & \ddots & \ddots & \ddots & \ddots & \ddots & \ddots & 0 \\
\vdots & \cdots & \cdots & \cdots & \cdots & 0 & \cdots & \cdots & 0 & (ik\Theta_{N-1}-1)e^{-ik(N-1)\epsilon} & -(ik\Theta_{N-1}+1) & e^{-ik(N-1)\epsilon} & e^{-ik\epsilon} \\
\vdots & \cdots & \cdots & \cdots & \cdots & \cdots & \cdots & \cdots & 0 & -ike^{-ik(N-1)\epsilon} & ik & ike^{ik(N-1)\epsilon} & ike^{ik\epsilon} \\
0 & \cdots & \cdots & \cdots & \cdots & \cdots & \cdots & \cdots & \cdots & \cdots & 0 & e^{-ikN\epsilon} & 1
\end{bmatrix}$$

$\widehat{G}$ has been introduced to establish a relationship between the spectral nodal displacements under boundary conditions $\widehat{u}_{\text{node}}$ and the constant coefficient matrix $\widehat{a}$. The expression of $\widehat{a}$ can be obtained from Eq. (4) as,

$$\widehat{a} = \widehat{G}^{-1}\,\widehat{u}_{\text{node}} = \widehat{\mathcal{F}}\,\widehat{u}_{\text{node}} \tag{5}$$

Applying boundary conditions on $\widehat{\mathcal{F}}$, the spectral stiffness matrix $\widehat{K}(\omega)$ of a multi-damage cantilever bar can be obtained as,

$$\widehat{K}(\omega) = EA_0\widehat{\mathcal{F}}(:,2N)^T \begin{bmatrix}
\int_0^{\epsilon} {s'_1}^T(x,\omega)s'_1(x,\omega)dx & \cdots & 0 \\
\vdots & \ddots & \vdots \\
\vdots & \int_{(p-1)\epsilon}^{p\epsilon} {s'_p}^T(x,\omega)s'_p(x,\omega)dx & \vdots \\
\vdots & \ddots & \vdots \\
0 & \cdots & \int_{(N-1)\epsilon}^{L} {s'_N}^T(x,\omega)s'_N(x,\omega)dx
\end{bmatrix} \widehat{\mathcal{F}}(:,2N) \tag{6}$$

2.2 Stochastic

2.2.1 Mathematical background of KL expansion

Any random process $S(x,\theta)$ with non-zero mean can be expressed as a sum of a deterministic part that contains the mean value $\mu_S(x) = \mathbb{E}\{S(x,\theta)\}$ of the concerned random process and a zero mean random process $Y(x,\theta)$ [9], and is given as

$$S(x,\theta) = \mu_S(x) + Y(x,\theta) \tag{7}$$

Here, x is a function of position vector with the domain D and θ is element of sample space of random events Ω [10]. The covariance function and the correlation function of $Y(x,\theta)$ is same as the covariance function of $S(x,\theta)$ and is denoted as $C_S(x_1,x_2)$. The simplest form of expressing a stochastic process is by using random polynomials and can be expressed as

$$f(x,\theta)=\sum_{k=0}^{q}\xi_k(\theta)x^k \tag{8}$$

where q is a finite value, ξ_k are uncorrelated random coefficients and x^k represents each element of parameter space. These random polynomials are difficult to analyze. To simplify the study, stationary processes are considered and mathematical background for random polynomials have been modified to cosine field. The representation of a complex random process as a summation of simple ones is complicated. Thus, the idea of orthogonal expansions have been introduced. Let $\{\varphi_n(x)\}$ be a set of functions on parameter space D and $\{\xi_n(\theta)\}$ be a set of uncorrelated random variables. The zero-mean random process can be written as

$$Y(x,\theta)=\sum_{n=1}^{\infty}\xi_n(\theta)\varphi_n(x) \tag{9}$$

The covariance function of the concerned zero-mean random process can be obtained as

$$\begin{aligned} C_s(x_1,x_2) &= \mathbb{E}\{Y(x_1,\theta)Y(x_2,\theta)\} \\ &= \sum_{m=1}^{\infty}\sum_{n=1}^{\infty}\varphi_m(x_1)\varphi_n(x_2)\mathbb{E}\{\xi_m(\theta)\xi_n(\theta)\}=\sum_{n=1}^{\infty}\varphi_n(x_1)\varphi_n(x_2) \end{aligned} \tag{10}$$

The above equation is obtained by considering the orthonormality property of $\{\xi_n(\theta)\}_n$, such that they can be considered as Hilbert space basis satisfying $\int \xi_n(\theta)\xi_m(\theta)d\theta=\delta_{mn}$, where δ_{mn} is the Kronecker delta.

Let the parameter set D be a compact domain such that $\lambda_1 \geq \lambda_2 \geq ...$ and $\psi_1,\psi_2,...$ are the ordered negative eigenvalues and corresponding normalized eigenfunctions of the covariance function $C_s(x_1,x_2)$, respectively. The space of square integrable functions on D to itself can be given in the integral form of Fredholm integral equation of second kind. This can be solved by eigenvalue and corresponding normalized eigenfunction pairs. The integral equation is given as

$$\int_D C_s(x_1,x_2)\psi_n(x_1)dx_1=\lambda_n\psi_n(x_2) \tag{11}$$

The KL expansion form can be achieved by applying Mercer's theorem. If the covariance function is symmetric, bounded and positive semi-definite then it can be expressed in uniformly convergent series expansion as

$$C_S(x_1,x_2)=\sum_{n=1}^{\infty}\lambda_n\psi_n(x_1)\psi_n(x_2) \tag{12}$$

An expression for ξ_n can be obtained by eliminating $C_S(x_1,x_2)$ from Eqs. (10) and (12), and is given as

$$\varphi_n=\sqrt{\lambda_n}\psi_n \tag{13}$$

Substituting Eq. (13) in (9), the KL expansion of $Y(x,\theta)$ can be obtained as

$$Y(x,\theta) = \sum_{n=1}^{\infty} \xi_n(\theta)\sqrt{\lambda_n}\psi_n(x) \tag{14}$$

provided $\xi_n(\theta)$ are independent and identically distributed and follows Gaussian distribution i.e. $\mathcal{N}(0,1)$. The final expression of a stochastic process in infinite terms of KL expansion is given as

$$S(x,\theta) = \mu_S(x) + \sum_{n=1}^{\infty} \xi_n(\theta)\sqrt{\lambda_n}\psi_n(x) \tag{15}$$

If the parameter space is replaced by a finite number of points then the infinite series expansion can be reduced to a truncated series of eigensolutions of the concerned covariance function. The analytical solution for all covariance functions are not available. However, the eigenvalue problems can be solved numerically. The beauty of KL expansion is that it can represent a random process by a finite number of terms known as the order ($\overline{N}$) of the KL expansion. The major advantage of the truncation is that it optimizes the truncation error for a given order. The final expression of a stochastic process is given by

$$\widehat{S}(x,\theta) = \mu_S(x) + \sum_{n=1}^{\overline{N}} \xi_n(\theta)\sqrt{\lambda_n}\psi_n(x) \tag{16}$$

2.2.2 Estimation of eigensolutions

Consider a one dimensional exponential decaying Gaussian covariance function. The covariance function is given by

$$C(x_1,x_2) = e^{\frac{-|x_1-x_2|}{b}} \tag{17}$$

where b is the correlation length. It is assumed that the analytical solution will be in the range $[-a < x < a]$ such that the mean is zero and produces the random field following Eq. (15). Based on Eq. (11), the Fredholm integral equation can be written as

$$\int_{-a}^{a} e^{-c|x_1-x_2|}\psi(x_2)dx_2 = \lambda\psi(x_1) \tag{18}$$

Considering $c = \frac{1}{b}$. Eq. (18) can be rewritten as

$$\int_{-a}^{x_1} e^{-c(x_1-x_2)}\psi(x_2)dx_2 + \int_{x_1}^{a} e^{-c(x_2-x_1)}\psi(x_2)dx_2 = \lambda\psi(x_1) \tag{19}$$

The first and second order derivative of the eigenfunctions with respect to x_1 can be obtained by applying Leibniz integral rule. Differentiating Eq. (19) twice with respect to x_1 and rearranging, the expression can be obtained as,

$$\psi''(x_1) = \frac{-2c+\lambda c^2}{\lambda}\psi(x_1) = \omega_k^2\psi(x_1)\ ,\left(\text{let } \omega_k^2 = \frac{-2c+\lambda c^2}{\lambda}\right) \tag{20}$$

Now, substituting $x_1 = -a$ and $x_1 = a$ and solving, the eigenvalues can be expressed as

$$\left[\omega_k^2 \geq 0; \tan(\omega_k a) = \frac{c}{\omega_k}\right] \cup \left[\omega_k^2 \geq 0; \tan(\omega_k a) = -\frac{\omega_k}{c}\right] \quad (21)$$

The graphical solution of Eq. (21) shows that $\tan(\omega_k a)$ takes decreasing sequence of positive and negative numbers for odd and even sequence of $\omega_k a$ respectively. The odd sequence corresponds to $\tan(\omega_k a) = \frac{c}{\omega_k}$ and the even sequence corresponds to $\tan(\omega_k a) = -\frac{\omega_k}{c}$. The eigenvalues can be obtained after determining ω_k by using

$$\lambda_j = \frac{2c}{c^2 - {\omega_k}_j^2}, j = 1, 2, 3 \ldots \quad (22)$$

The odd sequence of eigenvalues are obtained from,

$$\psi_j(x) = C_o \cos(\omega_{kj} x) \quad (23)$$

where C_o is a constant such that it satisfies

$$\int_{-a}^{a} C_o^2 \cos^2(\omega_{kj} x) dx = 1 \quad (24)$$

Thus normalizing the eigenfunction gives

$$C_o = \frac{1}{\sqrt{a + \frac{\sin(2\omega_{kj} a)}{2\omega_{kj}}}} \quad (25)$$

The corresponding eigenfunction is obtained as,

$$\psi_{jo}(x) = \frac{\cos(\omega_{kj} x)}{\sqrt{a + \frac{\sin(2\omega_{kj} a)}{2\omega_{kj}}}}, j = 1, 3, 5 \ldots \quad (26)$$

Similarly the even eigenvalues can be obtained from,

$$\psi_j(x) = C_e \sin(\omega_{kj} x) \quad (27)$$

where C_e is a constant such that it satisfies

$$\int_{-a}^{a} C_e^2 \sin^2(\omega_{kj} x) dx = 1 \quad (28)$$

Thus normalizing the eigenfunction gives

$$C_e = \frac{1}{\sqrt{a - \frac{\sin(2\omega_{kj} a)}{2\omega_{kj}}}} \quad (29)$$

The corresponding eigenfunction is obtained as,

$$\psi_{je}(x) = \frac{\sin(\omega_{kj} x)}{\sqrt{a - \frac{\sin(2\omega_{kj} a)}{2\omega_{kj}}}}, j = 2, 4, 6 \ldots \quad (30)$$

However for non-Gaussian stochastic field, the KL expansion can be applicable by modifying through memoryless transformation [11] involving cumulative distribution function of both the underlying Gaussian and target non-Gaussian distributions.

2.2.3 Stochastic expressions

Stochastic formulation of a vibrating rod is similar to the deterministic formulation but parameter like cross-section area (A_0), mass density (ρ), and Young's modulous of elasticity (E) may be assumed as spatially distributed random variables. The spectral stiffness for a cantilever bar-type structure considering material uncertainty can be expressed as

$$\widehat{K}_s(\omega,\theta) = \widehat{K}(\omega) + \varepsilon_1 \sum_{j=1}^{\overline{N}} \xi_{Kj}(\theta)\sqrt{\lambda_{Kj}}\widehat{K}_j(\omega) \tag{31}$$

where ε_1 indicates deterministic constant ranging between 0 and 1. $\widehat{K}(\omega)$ is the deterministic part as derived in Eq. (6). $\overline{N}$ is the number of terms of the truncated series in the KL expansion while $\xi_{Kj}(\theta)$ denotes uncorrelated Gaussian random variables with zero mean and unit standard deviation. Now based on the eigenvalues (λ_{Kj}) along with even and odd eigenfunctions i.e. Eqs. (26) and (30), the expressions of $\widehat{K}_j(\omega)$ can be obtained as,

$$\widehat{K}_j(\omega) = EA_0\widehat{\mathcal{F}}(:,2N)^T \begin{bmatrix} \int_0^{\epsilon} \psi_j {s'_1}^T(x,\omega)s'_1(x,\omega)dx & \cdots & 0 \\ \vdots & \ddots & \vdots \\ \vdots & \int_{(p-1)\epsilon}^{p\epsilon} \psi_j {s'_p}^T(x,\omega)s'_p(x,\omega)dx & \vdots \\ \vdots & \ddots & \vdots \\ 0 & \cdots & \int_{(N-1)\epsilon}^{L} \psi_j {s'_N}^T(x,\omega)s'_N(x,\omega)dx \end{bmatrix} \widehat{\mathcal{F}}(:,2N) \tag{32}$$

3 NUMERICAL SIMULATION

3.1 System specifications

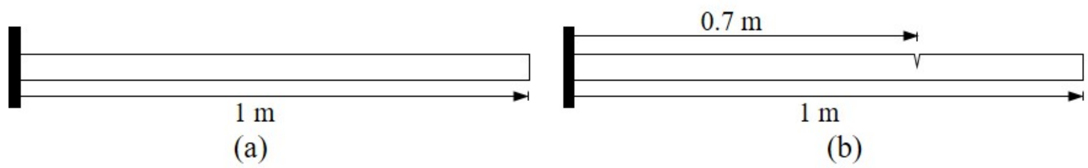

Figure 3: Cantilever bar: (a) undamaged and (b) damaged at 0.7m

Table 1: Details of system specifications

length (L)	1 m
cross-sectional area (A_0)	0.0003 m^2
Young's modulous (E)	200e9 Pa
mass density (ρ_0)	7850 kg/m^3

A cantilever bar has been modelled as shown in Fig 3. The structural specifications have been shown in table 1. Now for the damaged system, damage severity of 20% has been considered at 0.7 m from the fixed-end. Both deterministic as well stochastic analysis have been performed for undamaged and damaged system. In case of stochastic study both Gaussian and gamma distribution have been considered to generate the stochasticity in spectral stiffness of the undamaged system. However, only Gaussian distribution has been analysed in damaged

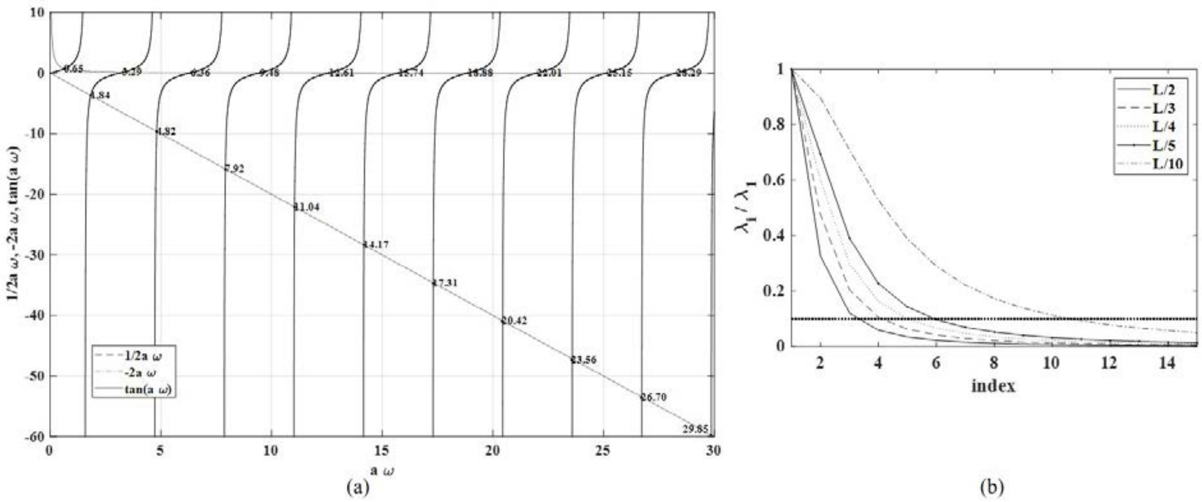

Figure 4: (a) Graphical solution of ω_k for even and odd terms and (b) Number of eigenvalues required to capture 90% of the stochastic field for different correlation lengths considering unit domain exponential covariance function

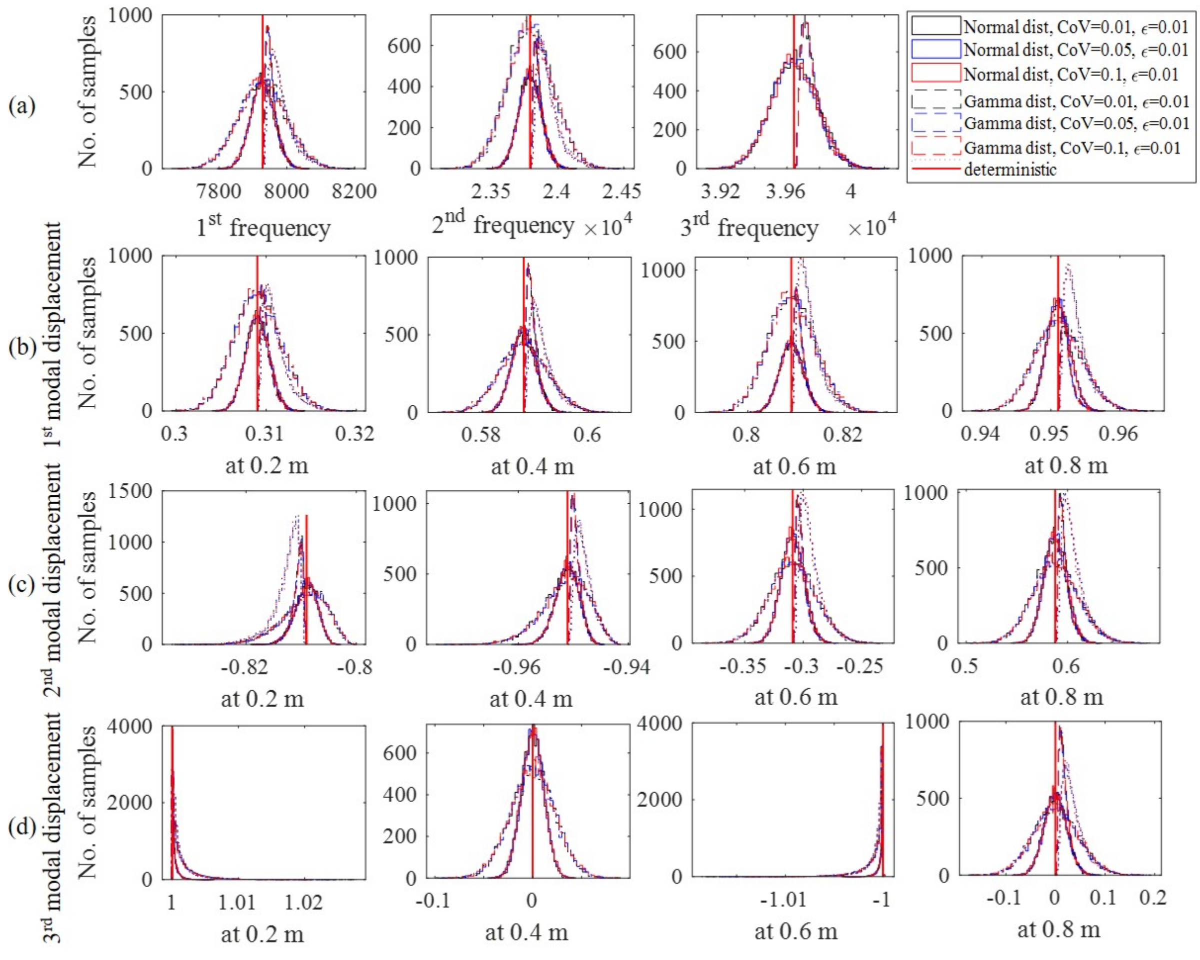

Figure 5: Distribution of responses due to different stochastic conditions in undamaged bar: (a) first three natural frequencies, (b) 1st, (c) 2nd and (d) 3rd modal displacements at 0.2, 0.4, 0.6 and 0.8 m from fixed-end, respectively.

bar. The coefficient of variation (CoV) of 0.01, 0.05 and 0.1 have been considered in the input randomness along with a deterministic constant (ϵ_1) of 0.01 for both undamaged and damaged system. A set of 20 random variables with zero mean and unit standard deviation has been considered for the Gaussian distribution. However for gamma distribution, memoryless transformation has been applied. Considering the correlation length $b = \frac{L}{2}$, the eigensolutions have been obtained as shown in Fig. 4(a). It has been observed from Fig. 4(b) that in case of this system, first 5 eigensolutions can capture 90% of the stochastic field [13]. The simulation study has been performed for 10000 samples for each case of damaged and undamaged system.

Normal, CoV=0.01, ε=0.01	mode 1					mode 2					mode 3				
	deter.	mean	CoV	skew.	kurt.	deter.	mean	CoV	skew.	kurt.	deter.	mean	CoV	skew.	kurt.
frequency	7928.7	7928.9	0.0043	0.0316	2.89	23786	23787	0.0036	0.0448	2.92	39643	39644	0.0035	0.0461	2.92
at 0.2 m	0.30902	0.30903	0.0042	0.0617	2.90	-0.80902	-0.80914	-0.0025	-0.3635	3.09	1	1.0004	0.0005	2.8027	15.06
at 0.4 m	0.58779	0.58781	0.0037	0.0611	2.90	-0.95106	-0.95116	-0.0022	-0.2681	3.02	2.32E-16	-8.61E-05	-129.54	-0.0464	2.93
at 0.6 m	0.80902	0.80904	0.0030	0.0600	2.90	-0.30902	-0.30898	-0.0312	0.0280	2.92	-1	-1.0002	-0.00035	-2.8021	15.06
at 0.8 m	0.95106	0.95108	0.0018	0.0584	2.90	0.58779	0.58789	0.0186	0.0607	2.92	-4.65E-16	0.000172	129.59	0.046356	2.93
Normal, CoV=0.05, ε=0.01	mode 1					mode 2					mode 3				
	deter.	mean	CoV	skew.	kurt.	deter.	mean	CoV	skew.	kurt.	deter.	mean	CoV	skew.	kurt.
frequency	7928.7	7928.3	0.0044	0.0249	2.98	23786	23785	0.0036	0.0421	2.99	39643	39642	0.0036	0.0422	3.00
at 0.2 m	0.30902	0.30901	0.0043	0.0569	2.98	-0.80902	-0.80912	-0.0025	-0.3798	3.18	1	1.0004	0.0005	2.7511	13.82
at 0.4 m	0.58779	0.58778	0.0038	0.0562	2.98	-0.95106	-0.95119	-0.0022	-0.2883	3.10	2.32E-16	7.96E-05	142.78	-0.04235	3.00
at 0.6 m	0.80902	0.80901	0.0030	0.0550	2.98	-0.30902	-0.30912	-0.0317	0.0244	2.99	-1	-1.0003	-0.00037	-2.7506	13.81
at 0.8 m	0.95106	0.95105	0.0018	0.0533	2.98	0.58779	0.58774	0.0189	0.0590	2.99	-4.65E-16	-0.00016	-142.72	0.042319	3.00
Normal, CoV=0.1, ε=0.01	mode 1					mode 2					mode 3				
	deter.	mean	CoV	skew.	kurt.	deter.	mean	CoV	skew.	kurt.	deter.	mean	CoV	skew.	kurt.
frequency	7928.7	7928.6	0.0044	0.0048	2.94	23786	23786	0.0037	0.0136	2.95	39643	39643	0.0036	0.0163	2.96
at 0.2 m	0.30902	0.30902	0.0043	0.0363	2.94	-0.80902	-0.80913	-0.0025	-0.3454	3.09	1	1.0004	0.0005	2.6775	13.08
at 0.4 m	0.58779	0.58779	0.0038	0.0356	2.94	-0.95106	-0.95118	-0.0022	-0.3122	3.08	2.32E-16	3.12E-06	3661.9	-0.01633	2.96
at 0.6 m	0.80902	0.80902	0.0030	0.0345	2.94	-0.30902	-0.30905	-0.0319	-0.0039	2.95	-1	-1.0003	-0.00036	-2.6771	13.07
at 0.8 m	0.95106	0.95106	0.0018	0.0328	2.94	0.58779	0.58781	0.0190	0.0302	2.95	-4.65E-16	-6.26E-06	-3647.8	0.016327	2.96
gamma, CoV=0.01, ε=0.01	mode 1					mode 2					mode 3				
	deter.	mean	CoV	skew.	kurt.	deter.	mean	CoV	skew.	kurt.	deter.	mean	CoV	skew.	kurt.
frequency	7928.7	7956	0.002233	1.3186	5.0032	23786	23858	0.001855	1.3559	5.1817	39643	39761	0.00184	1.3585	5.1855
at 0.2 m	0.30902	0.31005	0.002185	1.3374	5.086	-0.80902	-0.81079	-0.00144	-1.5438	6.0802	1	1.0004	0.000487	3.1876	17.984
at 0.4 m	0.58779	0.58955	0.001955	1.337	5.0842	-0.95106	-0.94941	-0.00099	1.1392	4.2762	2.32E-16	-0.00931	-0.62409	-1.3642	5.2147
at 0.6 m	0.80902	0.81094	0.001548	1.3363	5.0811	-0.30902	-0.30095	-0.01652	1.3471	5.1433	-1	-1.0002	-0.00032	-3.187	17.977
at 0.8 m	0.95106	0.9524	0.000923	1.3353	5.0766	0.58779	0.597	0.009572	1.3676	5.2359	-4.65E-16	0.018616	0.62395	1.3633	5.2098
gamma, CoV=0.05, ε=0.01	mode 1					mode 2					mode 3				
	deter.	mean	CoV	skew.	kurt.	deter.	mean	CoV	skew.	kurt.	deter.	mean	CoV	skew.	kurt.
frequency	7928.7	7955.9	0.002264	1.3799	5.2696	23786	23857	0.001879	1.419	5.4576	39643	39760	0.001865	1.4223	5.4633
at 0.2 m	0.30902	0.31005	0.002216	1.3998	5.3584	-0.80902	-0.81079	-0.00146	-1.617	6.4105	1	1.0004	0.000502	3.2861	18.107
at 0.4 m	0.58779	0.58954	0.001982	1.3993	5.3565	-0.95106	-0.94942	-0.00101	1.1894	4.4835	2.32E-16	-0.00928	-0.63471	-1.4284	5.4945
at 0.6 m	0.80902	0.81093	0.00157	1.3986	5.3531	-0.30902	-0.30097	-0.01673	1.4098	5.4166	-1	-1.0002	-0.00033	-3.2856	18.101
at 0.8 m	0.95106	0.9524	0.000936	1.3975	5.3483	0.58779	0.59697	0.0097	1.4315	5.5155	-4.65E-16	0.018549	0.63456	1.4274	5.4892
gamma, CoV=0.1, ε=0.01	mode 1					mode 2					mode 3				
	deter.	mean	CoV	skew.	kurt.	deter.	mean	CoV	skew.	kurt.	deter.	mean	CoV	skew.	kurt.
frequency	7928.7	7956	0.002269	1.3365	5.0325	23786	23858	0.001888	1.3685	5.1859	39643	39761	0.001872	1.3736	5.199
at 0.2 m	0.30902	0.31005	0.002221	1.3555	5.1139	-0.80902	-0.81079	-0.00147	-1.5566	6.0523	1	1.0004	0.000499	3.1469	16.775
at 0.4 m	0.58779	0.58955	0.001987	1.3551	5.1121	-0.95106	-0.94941	-0.00101	1.1498	4.2976	2.32E-16	-0.00931	-0.63484	-1.3794	5.2271
at 0.6 m	0.80902	0.81094	0.001573	1.3544	5.1091	-0.30902	-0.30094	-0.01681	1.3596	5.1485	-1	-1.0002	-0.00033	-3.1465	16.77
at 0.8 m	0.95106	0.9524	0.000938	1.3534	5.1047	0.58779	0.597	0.009743	1.3803	5.2385	-4.65E-16	0.018616	0.6347	1.3784	5.2223

Figure 6: Statistical indicators obtained from modal parameters due to different stochastic conditions in undamaged system

3.2 Results and discussion

The material uncertainty propagates into the modal parameters of any system. In this study, the first three natural frequencies and the modal displacements at 0.2, 0.4, 0.6 and 0.8 m from the fixed end of both the damaged and undamaged bar have been determined. The probability distribution corresponding to the undamaged system considering material randomness as Gaussian and gamma distribution has been shown in Fig. 5. The statistical indicators namely, mean, standard deviation, CoV, skewness and kurtosis for all samples have been considered as the key parameters for describing the randomness in response parameters. The statistical results corresponding to the undamaged bar has been presented in Fig. 6. Similarly, for the damaged bar element, the study has been performed considering only the Gaussian randomness as the material uncertainty. The probability distributions and the statistical indicators of the damaged system have been shown in Figs. 7 and 8, respectively. It has been observed that as the modal displacement gets closer to zero crossing of any mode shape, the skewness increases. Again in most of the cases of Gaussian randomness in material, the kurtosis is around 3 as should be in Gaussian distribution. Whereas, in case of material uncertainty as gamma distribution, the obtained kurtosis is mostly around 5. Some discrepancies have been observed in determination of fundamental frequency of the damaged system which requires modifications. Again, the uncertainty propagation in the damage quantification need to be studied along with the variation in mode shape difference and damage severity due to various input uncertainty.

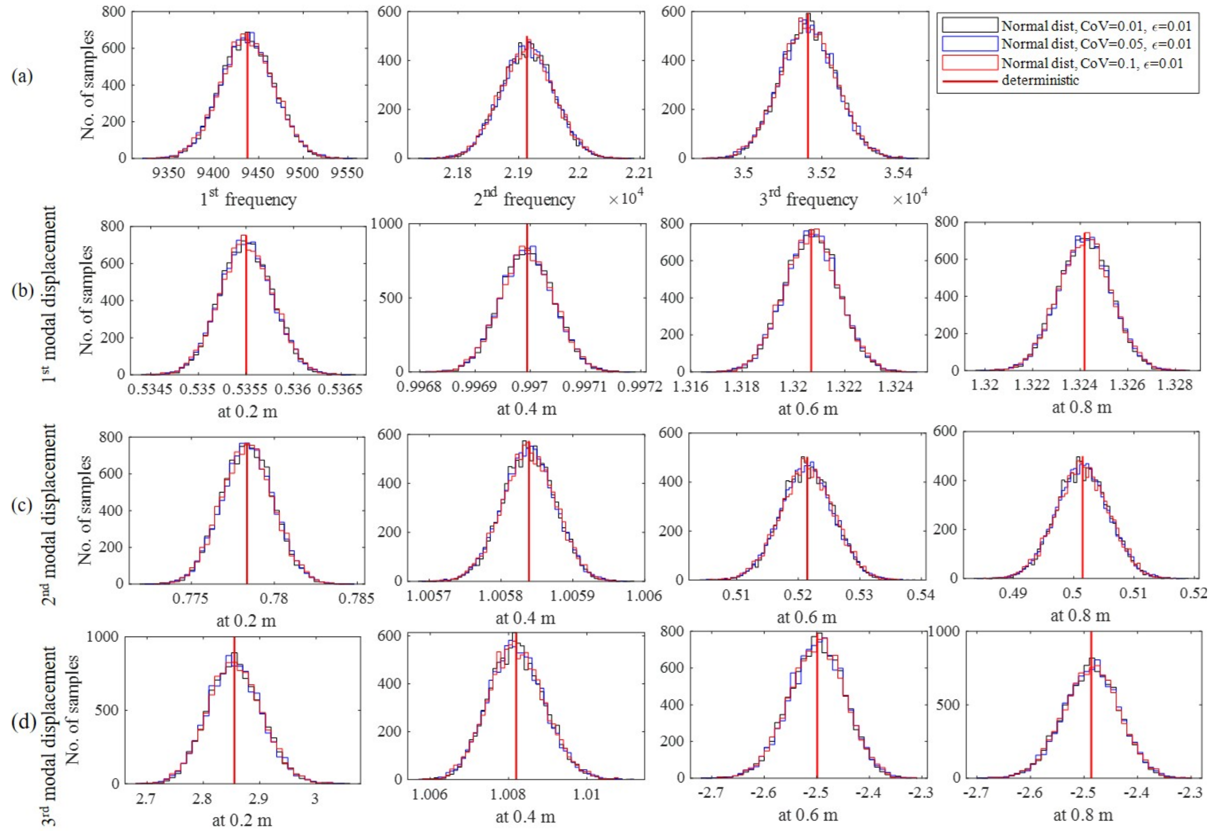

Figure 7: Distribution of responses due to different stochastic conditions in damaged bar: (a) first three natural frequencies, (b) 1st, (c) 2nd and (d) 3rd modal displacements at 0.2, 0.4, 0.6 and 0.8 m from fixed-end, respectively.

Normal, CoV=0.01 , ε=0.01	mode 1					mode 2					mode 3				
	deter.	mean	CoV	skew.	kurt.	deter.	mean	CoV	skew.	kurt.	deter.	mean	CoV	skew.	kurt.
frequency	9437.4	9437.4	0.003151	0.018758	2.9327	21914	21914	0.001969	-0.00678	2.9272	35164	35164	0.002044	0.034104	2.9297
at 0.2 m	0.5355	0.5355	0.00051	0.029416	2.9332	0.77835	0.77836	0.001984	0.008457	2.928	2.8551	2.8562	0.016595	0.13317	2.9604
at 0.4 m	0.99699	0.99699	4.77E-05	0.019705	2.9326	1.0058	1.0058	3.60E-05	-0.0322	2.9299	1.0082	1.0082	0.000699	0.16452	2.9754
at 0.6 m	1.3207	1.3207	0.00079	-0.02886	2.9332	0.52146	0.52143	0.008086	-0.00171	2.9275	-2.4991	-2.5002	-0.02112	-0.12299	2.956
at 0.8 m	1.4159	1.3242	0.000827	-0.02868	2.9331	0.10443	0.50146	0.008517	-0.0013	2.9275	-2.8616	-2.4875	-0.02083	-0.12288	2.956
Normal, CoV=0.05 , ε=0.01	mode 1					mode 2					mode 3				
	deter.	mean	CoV	skew.	kurt.	deter.	mean	CoV	skew.	kurt.	deter.	mean	CoV	skew.	kurt.
frequency	9437.4	9437.1	0.003207	0.014415	2.9961	21914	21914	0.002005	-0.00433	2.9909	35164	35163	0.002074	0.01709	2.9862
at 0.2 m	0.5355	0.5355	0.000519	0.025619	2.9964	0.77835	0.77838	0.002019	0.011686	2.9921	2.8551	2.8554	0.016828	0.12053	3.014
at 0.4 m	0.99699	0.99699	4.86E-05	0.015415	2.996	1.0058	1.0058	3.67E-05	-0.03658	2.9947	1.0082	1.0082	0.000708	0.1533	3.0283
at 0.6 m	1.3207	1.3207	0.000804	-0.02503	2.9964	0.52146	0.52139	0.008232	-0.00459	2.9914	-2.4991	-2.4993	-0.02142	-0.1099	3.0099
at 0.8 m	1.4159	1.3242	0.000841	-0.02484	2.9964	0.10443	0.50141	0.00867	-0.00416	2.9914	-2.8616	-2.4866	-0.02113	-0.10979	3.0099
Normal, CoV=0.1, ε=0.01	mode 1					mode 2					mode 3				
	deter.	mean	CoV	skew.	kurt.	deter	mean	CoV	skew.	kurt.	deter.	mean	CoV	skew.	kurt.
frequency	9437.4	9437.3	0.003226	-0.01633	2.957	21914	21914	0.002019	0.03048	2.9539	35164	35164	0.002079	0.00266	2.9571
at 0.2 m	0.5355	0.5355	0.000522	-0.00528	2.956	0.77835	0.77837	0.002034	0.046311	2.9568	2.8551	2.8557	0.016874	0.10468	2.9737
at 0.4 m	0.99699	0.99699	4.89E-05	-0.01534	2.9568	1.0058	1.0058	3.69E-05	-0.07095	2.9621	1.0082	1.0082	0.00071	0.13697	2.9843
at 0.6 m	1.3207	1.3207	0.000808	0.005858	2.9561	0.52146	0.52142	0.008291	-0.0393	2.9554	-2.4991	-2.4997	-0.02148	-0.09421	2.9708
at 0.8 m	1.4159	1.3242	0.000846	0.006048	2.9561	0.10443	0.50144	0.008732	-0.03888	2.9553	-2.8616	-2.487	-0.02119	-0.0941	2.9707

Figure 8: Statistical indicators obtained from modal parameters due to different stochastic conditions in damaged system

4 CONCLUSION

In this study, a detailed literature survey regarding the appropriate probability distribution to model material uncertainty has been conducted. A detailed derivation of KL expansion has been described for modelling stochasticity in material properties of any system. It has been then applied to obtain the closed-form expression of spectral stiffness for a multi-damaged cantilever bar-type structure. Extensive simulation study has been performed on both undamaged and damaged bar-type system to understand the propagation of material uncertainty in the modal parameters. Both Gaussian and gamma distribution-based randomness have been introduced as input in the undamaged system. However in case of damaged system, only Gaussian distribution has been followed as material uncertainty. Statistical indicators have been determined to understand the uncertainty propagation in the structural responses. However, the study may be further extended in quantifying multi-damage in bar-type systems as well as in real civil structures.

REFERENCES

[1] S. Mahadevan, A. Haldar, *Probability, reliability and statistical method in engineering design* . John Wiley & Sons, 2000.

[2] C. Soize, *An Accelerated Course with Advanced Applications in Computational Engineering, Vol. 47 of Interdisciplinary Applied Mathematics* . John Wiley & Sons, 2000.

[3] Y. Liu, S.T. Quek, F. H. Lee, Translation random field with marginal beta distribution in modeling material properties. *Structural Safety* , **61**, 57–66, 2016.

[4] Y. Liu, M.D. Shields, A direct simulation method and lower-bound estimation for a class of gamma random fields with applications in modelling material properties. *Probabilistic Engineering Mechanics*, **47**, 16–25, 2017.

[5] P. E. Hess, D. Bruchman, I. A. Assakkaf, B. M. Ayyub, Uncertainties in material and geometric strength and load variables. *Naval engineers journal* , **114**, 139–166, 2002.

[6] S. Shahinur, *Quantification of uncertainty of material properties and its application* , 2018.

[7] B. S. Grewal, *Higher engineering mathematics* . Khanna Publishers, New Delhi, 2002.

[8] S. Rahman, H. Xu, A meshless method for computational stochastic mechanics. *International Journal for Computational Methods in Engineering Science and Mechanics* , **6**, 41–58, 2005.

[9] M. Schevenels, G. Lombaert, G. Degrande, Application of the stochastic finite element method for Gaussian and non-Gaussian systems. *ISMA2004 International Conference on Noise and Vibration Engineering* , 3299–3314, 2004.

[10] R. G. Ghanem, P. D. Spanos, *Stochastic finite elements: a spectral approach* . Courier Corporation, 2003.

[11] M.R. Machado, S. Adhikari, J.M.C. Dos Santos, A spectral approach for damage quantification in stochastic dynamic systems. *Mechanical Systems and Signal Processing* , **88**, 253–273, 2017.

[12] B. Basu, D. Tiwari, D. Kundu, R. Prasad, Is Weibull distribution the most appropriate statistical strength distribution for brittle materials? *Ceramics International* , **35**, 237–246, 2009.

[13] S. Adhikari, M. I. Friswell, Distributed parameter model updating using the Karhunen–Loève expansion. *Mechanical systems and signal processing*, **24**, 326–339, 2010.